Inscuteable and NuMA proteins bind competitively to Leu-Gly-Asn repeat-enriched protein (LGN) during asymmetric cell divisions

Simone Culurgioni, Andrea Alfieri, Valentina Pendolino, Federica Laddomada, and Marina Mapelli[1]

Department of Experimental Oncology, European Institute of Oncology, Via Adamello 16, 20139 Milan, Italy

Edited by Terry L. Orr-Weaver, Whitehead Institute, Cambridge, MA, and approved September 29, 2011 (received for review August 9, 2011)

Coupling of spindle orientation to cellular polarity is a prerequisite for epithelial asymmetric cell divisions. The current view posits that the adaptor Inscuteable (Insc) bridges between Par3 and the spindle tethering machinery assembled on NuMA:LGN:Gαi^{GDP}, thus triggering apico-basal spindle orientation. The crystal structure of the Drosophila ortholog of LGN (known as Pins) in complex with Insc reveals a modular interface contributed by evolutionary conserved residues. The structure also identifies a positively charged patch of LGN binding to an invariant EPE-motif present on both Insc and NuMA. In vitro competition assays indicate that Insc competes with NuMA for LGN binding, displaying a higher affinity, and that it is capable of opening the LGN conformational switch. The finding that Insc and NuMA are mutually exclusive interactors of LGN challenges the established model of force generators assembly, which we revise on the basis of the newly discovered biochemical properties of the intervening components.

Asymmetric cell divisions regulate the position and the fate choice of daughter cells, with impact on numerous phenotypes of multicellular organisms. During development, asymmetric divisions coordinate cell growth with cell specification to determine tissue morphogenesis, while in adult life they sustain tissue homeostasis and regeneration (1). In asymmetric divisions specific cortical landmarks instruct the orientation of the mitotic spindle to promote unequal partitioning of fate determinants in cellular systems as diverse as *Caenorhabditis elegans* zygotes, *Drosophila* neuroblasts, as well as vertebrate skin and neural progenitors (2). Spindle coupling to polarity cues involves the recruitment at cortical sites of molecular devices, known as *force generators*, whose main task is to capture astral microtubules emanating from the spindle poles and to establish pulling forces. Core components of force generators are the evolutionary conserved NuMA:LGN:Gαi complexes, termed Mud:Pins:Gαi in flies. Topologically, tetratricopeptide repeats (TPR) present in the N-terminal portion of LGN mediate the interactions with NuMA, while GoLoco motifs at the C terminus serve as a docking platform for four Gαi^{GDP} subunits anchored at the plasma membrane via a myristoyl group (3). LGN exclusively binds to GDP-loaded Gαi (4). The association of cortical NuMA with the microtubule motor Dynein/Dynactin (5) provides a sliding anchorage for depolymerizing microtubules, whose shrinkage pulls towards the cortex the connected spindle pole. FRET studies revealed that LGN behaves as a conformational switch held in a closed form in interphase by head-to-tail interactions (3).

An issue intimately related to how force generators are assembled is how they are recruited at sites of polarization. In polarized asymmetric divisions, the apico-basal polarity axis is established by the asymmetrical distribution of Par3:Par6:aPKC at the apical cortex, which are able to recruit NuMA:LGN:Gαi^{GDP} via an adaptor named Inscuteable (Insc) (6). Insc was first identified in larval *Drosophila* neuroblasts as a partner of Par3 (Bazooka in flies) colocalizing with polarity proteins right after delamination (7–9), and later shown to bind Pins (10). Mammalian Insc homologues endowed with similar properties have been discovered in rat retina (11) and in mouse developing skin (12). Insc overexpression is sufficient to induce apico-basal divisions in cells that normally divide in a planar fashion such as *Drosophila* embryonic ephitelial cells (7), vertebrate neuroepithelial progenitors (13), and mouse skin progenitors (6). The portion of fly Insc encompassing residues 252–615 recapitulates Insc functions in neuroblasts (hence termed "asymmetric domain"), and directly interacts with Pins (9). Based on its interaction with both Par3 and LGN, Insc has been considered the molecular link between cortical Par proteins and NuMA:LGN:Gαi^{GDP} complexes. This notion is mainly substantiated by imaging analyses conducted in fly neuroblasts and mouse skin progenitors showing that during asymmetric metaphases Par3, Insc, LGN, and NuMA colocalyze in a cortical region underlying one of the spindle poles (1, 6, 12). However, no proof has been provided for the simultaneous association of LGN with Insc and NuMA, which remains a key question to elucidate how force generators work. We thus set out to study how LGN interacts with Insc and NuMA.

Results

Determination of the Crystal Structure of Pins:Insc. Human Insc:LGN:Gαi^{GDP} was refractory to crystallization. We thus took advantage of the functional information available on fruitfly proteins (Fig. 1*A*), and generated a dicistronic vector for coexpression in bacteria in which we cloned the TPR repeats and part of the linker region of Pins (Pins$^{TPR\text{-}LINKER}$) fused with a GST moiety in the first cassette, and a fragment corresponding to the asymmetric domain of Insc (Insc^{ASYM}) in the second cassette. This strategy yielded a soluble Pins$^{TPR\text{-}LINKER}$:Insc^{ASYM} complex eluting from a size exclusion chromatography (SEC) as a monodisperse sample (Fig. 1*B*). In order to obtain diffraction quality crystals, we had to further shorten these Pins and Insc constructs by limited proteolysis. When subjected to trypsinization, both subunits of Pins$^{TPR\text{-}LINKER}$:Insc^{ASYM} were trimmed to smaller fragments (Fig. S1), which were assigned by mass spectrometry to Pins$^{25–406}$ and Insc$^{303–340}$ respectively. SEC analysis confirmed that Pins$^{25–406}$ stably associates with Insc$^{303–340}$ with a 1:1 stoichiometry (Fig. 1*B*). To gain an understanding of the organizational principles of the interaction, we determined the structure of the proteolitically defined Pins$^{25–406}$:Insc$^{303–340}$ complex, referred to as Pins^{TPR}:dInsc^{PEPT} (where "d" stands for *Drosophila*).

To determine the crystallographic structure, we used SAD phases from selenomethionine-substituted protein crystals. The

Author contributions: S.C. and M.M. designed research; S.C., A.A., V.P., and F.L. performed research; S.C. and M.M. analyzed data; and M.M. wrote the paper.

The authors declare no conflict of interest.

This article is a PNAS Direct Submission.

Data deposition: The atomic coordinates have been deposited to the Protein Data Bank www.pdb.org (PDB ID code 4A1S).

[1]To whom correspondence should be addressed. E-mail: marina.mapelli@ifom-ieo-campus.it.

This article contains supporting information online at www.pnas.org/lookup/suppl/doi:10.1073/pnas.1113077108/-/DCSupplemental.

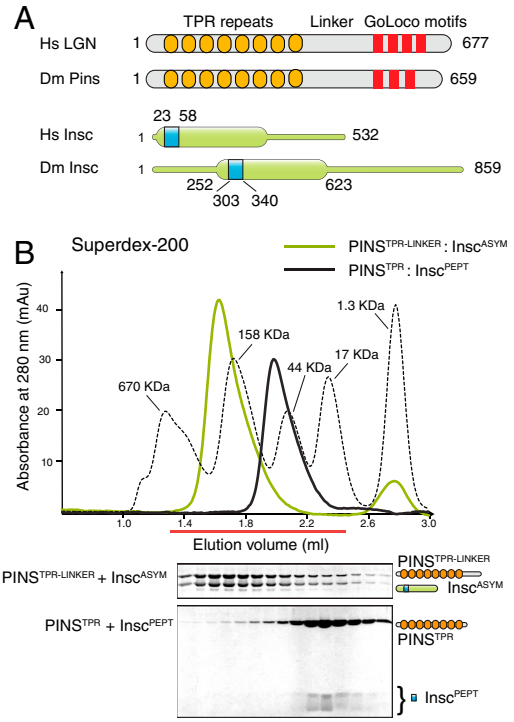

Fig. 1. Generation of the Pins:Insc complex. (*A*) Scheme of LGN and Insc. (*B*) SEC elution profiles of $Pins^{TPR-LINKER}$:$Insc^{ASYM}$ and $Pins^{TPR}$:$dInsc^{PEPT}$.

structure has been refined to 2.1 Å resolution with an R_{free} of 25.6% (Table S1). The final model includes residues 307 to 335 of dInsc peptide, and residues 39–386 of Pins.

General Architecture of the Pins:Insc Assembly. The $Pins^{TPR}$ domain folds into a cradle-shaped arch harboring the extended $dInsc^{PEPT}$ into its inner concave surface (Fig. 2 *A*–*C*). In such arrangement, the Pins and dInsc polypeptide chains run with opposite direction, with the helical N terminus of $dInsc^{PEPT}$ contacting the C-terminal portion of $Pins^{TPR}$. Spiraling of the $Pins^{TPR}$ domain around $dInsc^{PEPT}$ generates an extensive interaction surface of about 1,900 $Å^2$, corresponding to approximately 50% of the $dInsc^{PEPT}$ surface area.

The $Pins^{TPR}$ domain consists of 17 antiparallel helices forming 8.5 TPR repeats (Fig. S2), with a pattern of hydrophobic amino acids consistent with the canonical TPR consensus (14). The sequence 39–76 adopts a TPR-like arrangement despite deviating from the consensus. In addition, the fourth TPR repeat presents an insertion between the first and the second helix (Fig. S2) resulting in longer α4A and α4B helices joined by a 8-residue loop. Consecutive TPR units stack in much the same way as reported for the TPR-containing domain of O-linked N-actylglucosamine transferase (15), giving rise to a right-handed superhelical twist of the molecule. The unusual sequence composition of the TPR4 repeat distorts the superhelix by an outward displacement of the subsequent TPR units with respect to the helical axis (see Fig. S3).

A peculiar aspect of the $Pins^{TPR}$ structure is the presence within the groove of a set of asparagines positioned on the third and fourth turn of the αA helix of each TPR repeat, which generate a ridge extending throughout the concave surface of the molecule (Fig. 2*D*). These asparagine residues occupy the positions 6 and 9 of the TPR consensus, within an invariant *NLGN* motif found in most of the Pins TPR repeats. Not surprisingly, in the binary complex $dInsc^{PEPT}$ lines up with this asparagine ladder. This binding mode is reminiscent of the binding of similarly extended ligands to multiple ARM-repeat proteins such as the NLS peptides bound to karyopherin α (16), and the E-cadherin peptide bound to β-catenin (17), thus suggesting a general recognition mechanism common to all these topologically diverse helical scaffolds.

Determinants of Interactions Between Pins and Insc. We next addressed the structural determinants of the $Pins^{TPR}$:$dInsc^{PEPT}$ assembly. As expected for TPR repeat-containing proteins, the hetero-dimer interface is contributed by the amino acids of the αA helices, facing the inner side of the domain. To facilitate the

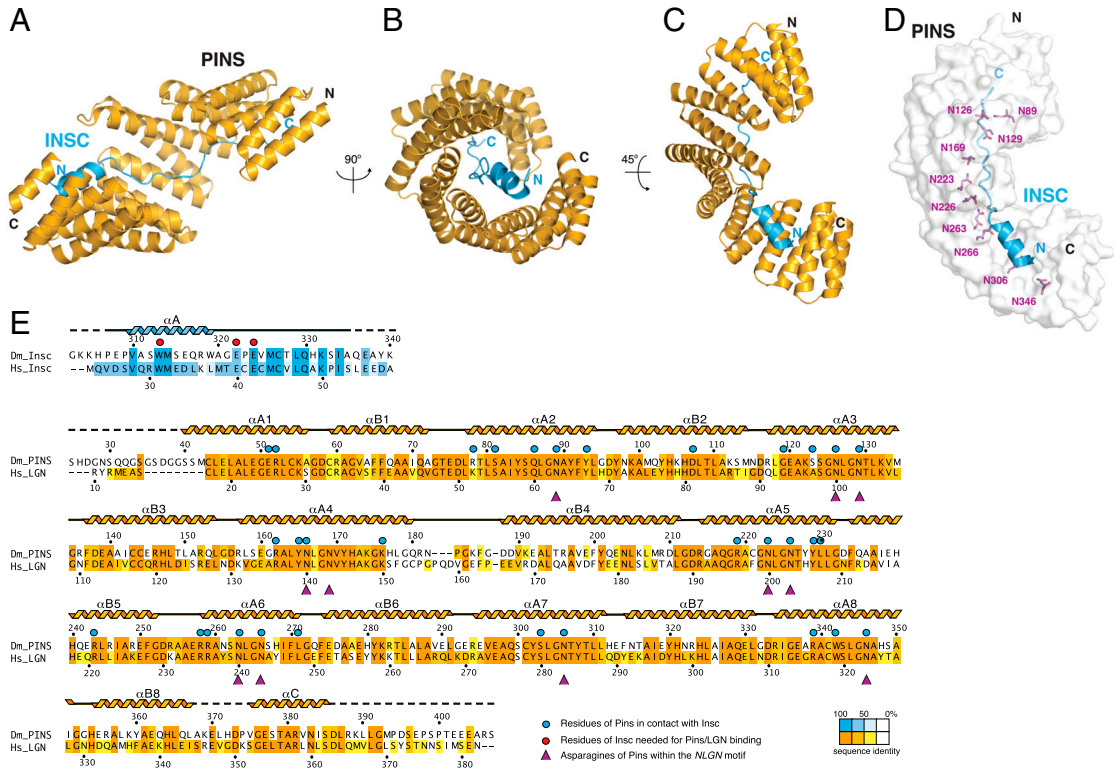

Fig. 2. Structure of the $Pins^{TPR}$:$dInsc^{PEPT}$ dimer. (*A*–*C*) Ribbon models of the $Pins^{TPR}$:$dInsc^{PEPT}$ complex viewed at the indicated orientations. (*D*) Surface representation of $Pins^{TPR}$ with the $dInsc^{PEPT}$ lining along the conserved asparagines (purple). (*E*) Sequence and secondary structure of $Pins^{TPR}$ and $dInsc^{PEPT}$ colored according to the conservation.

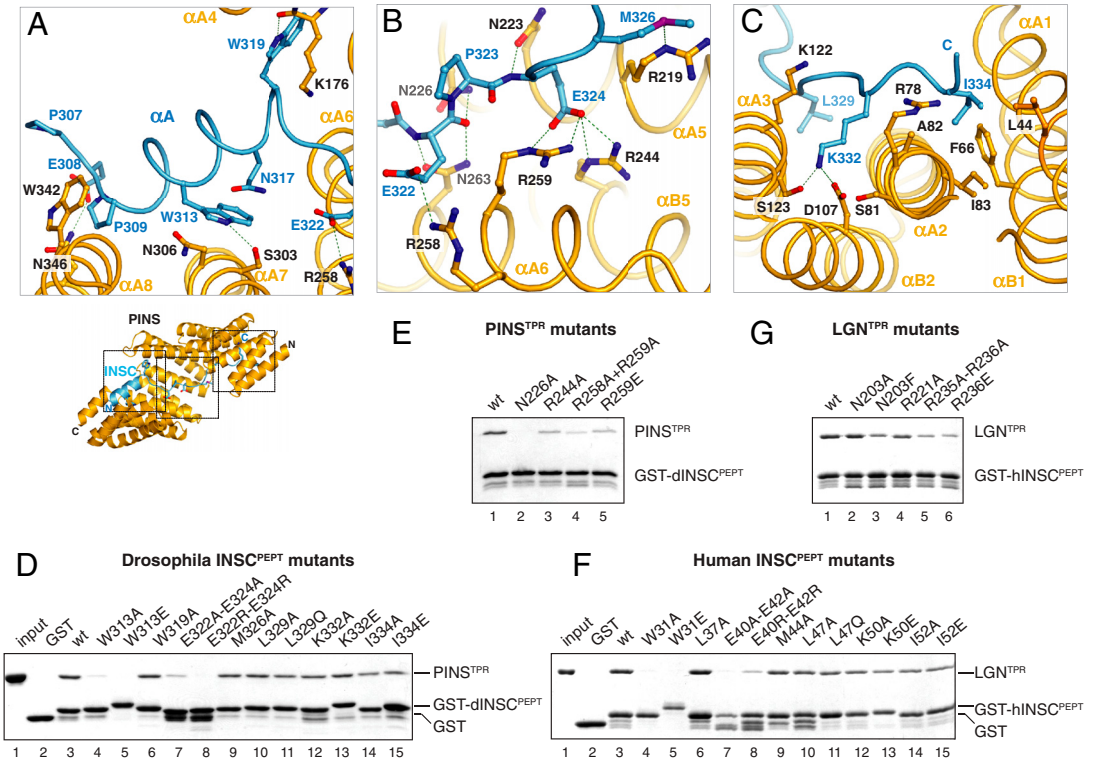

Fig. 3. Analysis and conservation of the Pins^{TPR}:dInsc^{PEPT} dimer interface. (*A*–*C*) Enlarged views of the dimer interface. (*D*) GST-dInsc^{PEPT}, mutated as indicated above, on GSH beads was incubated with Pins^{TPR}. After washing species on beads were analyzed by SDS-PAGE. (*E*) Binding of Pins^{TPR} mutants to wt-dInsc^{PEPT}. (*F* and *G*) Same assays as in boxes *D* and *E* performed with human LGN^{TPR} and hInsc^{PEPT}.

description, we will divide the interactions into three major modules roughly matching the dInsc^{PEPT} N-terminal α-helix, the central E322-P323-E324^{Insc} motif, and the elongated C-terminal stretch. The first module involves the helix αA of dInsc^{PEPT} that packs against the TPR repeats 6 and 7 of Pins^{TPR} with an orientation almost perpendicular to the repeats' axis (Fig. 3*A*). This helix contains the invariant Trp313^{Insc} that is hydrogen-bonded to Ser303^{Pins} and further stabilized by stacking interactions with Asn306^{Pins}. The correct orientation of the αA helix is ensured on one end by a hydrogen bond between Glu308^{Insc} and Asn346^{Pins}, and on the other end by the hydrogen bond between the Trp319^{Insc} and the carbonyl group of Lys176^{Pins} located in the TPR4 insertion. At Trp319^{Insc} the dInsc^{PEPT} chain turns sharply to progress parallel to the αA5 helix of Pins^{TPR} until Met326^{Insc}, crossing the whole surface of the TPR domain (Fig. 3*B*). Hydrogen bonds from the conserved asparagines Asn223^{Pins}, Asn226^{Pins}, and Asn263^{Pins} anchor the dInsc^{PEPT} main chain to the TPR scaffold, and a number of salt bridges between Glu322^{Insc} and Glu324^{Insc} and Arg244^{Pins}, Arg258^{Pins} and Arg259^{Pins} greatly contribute to strengthen the interaction. The electrostatic potential of the Pins^{TPR} surface in this area confirms that the negatively charged EPE^{Insc} triplet is accommodated into a positively charged patch of the central portion of the Pins^{TPR} domain (Fig. S4), thus suggesting that charge complementarity might constitute the major factor dictating the ligand specificity here. The third area of interactions involves the C-terminal end of dInsc^{PEPT} and the first three TPR units of Pins^{TPR}. This portion of dInsc^{PEPT} inserts the side chains of Lys332^{Insc} and Ile334^{Insc} into two adjacent pockets at opposite sites of the helix (Fig. 3*C*). Lys332^{Insc} snugly fits into the negatively charged cavity formed by Ser81^{Pins}, Ser123^{Pins}, and Asp107^{Pins}, whereas Ile334^{Insc} sits into a predominantly hydrophobic environment contributed by Leu44^{Pins}, Phe66^{Pins}, and Ile83^{Pins}.

To address the relevance of each interaction module for the dimer assembly, we substituted key residues identified by our structural analysis. The binding ability of the mutated proteins was tested in a pull-down assay performed with GST-dInsc^{PEPT} immobilized onto glutathione sepharose (GSH) beads and purified Pins^{TPR} constructs in solution. We first asked if dInsc^{PEPT} mutants were able to bind wild-type Pins^{TPR} (Fig. 3*D*). As expected, double replacement of E322-E324^{Insc} with alanine or arginine fully abrogates the binding. The same effect is caused by substitution of the Trp313^{Insc} with alanine or glutamic acid, underscoring a fundamental role of this triptophane in docking the dInsc^{PEPT} helical fragment onto Pins^{TPR}. Mutations of Trp319^{Insc}Ala and Met326^{Insc}Ala, as well as substitution of the invariant residues Leu329^{Insc}, Lys332^{Insc}, and Ile334^{Insc} on the dInsc^{PEPT} C terminus do not severely affect binding. We next tested the structural determinants of the binding on the Pins^{TPR} side, focusing our mutational analysis on the central EPE^{Insc} module. In keeping with the role predicted for the invariant asparagines of Pins^{TPR} in anchoring the dInsc^{PEPT} backbone, removal of the Asn226^{Pins} side chain is sufficient to abolish binding (Fig. 3*E*). Single mutations of Arg244^{Pins} and Arg259^{Pins} to alanine or glutamic acid strongly reduce binding, while double substitution of Arg258^{Pins} and Arg259^{Pins} with alanine results in a Pins^{TPR} mutant unable to associate with dInsc^{PEPT}. In summary, our results indicate that; (*i*) all three dInsc^{PEPT} portions including the N-terminal α-helix, the central EPE^{Insc} motif, and the extended C-terminal tail synergize in binding Pins^{TPR}; (*ii*) the polar interactions between the negative charges of the EPE^{Insc} motif and the positively charged inner surface of Pins^{TPR} is a hallmark of dInsc^{PEPT} recognition; (*iii*) besides Glu322^{Insc} and Glu324^{Insc}, a key determinant of the dimeric assembly is the invariant Trp313^{Insc}.

The Pins:Insc Interface Is Evolutionary Conserved. One of the open questions in the stem cell field is to which extent the molecular mechanisms underlying *Drosophila* neuroblast divisions are conserved in vertebrates. To gain insight into this issue, we generated constructs of human LGN and Insc corresponding to the fruitfly domains we had used for the structure determination, and repeated the GST pull-down assays with an analogous battery of mutants. Sequence analysis revealed that the counterparts of the dInsc^{PEPT} spans residues 23 to 58 of the human Insc, to which we refer as hInsc^{PEPT}, where "h" stands for *h*uman. As predicted

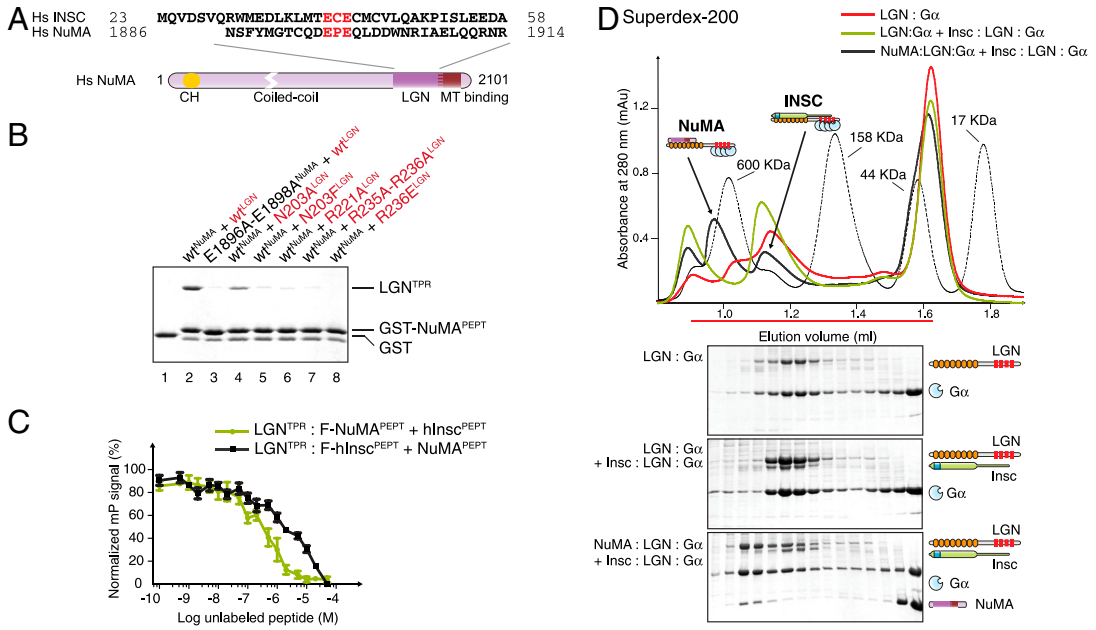

Fig. 4. NuMA competes with Insc for the binding to LGN via the invariant EPE motif. (*A*) Alignment of hInscPEPT and NuMAPEPT around the conserved ECE/EPE motif. (*B*) Validation of the NuMAPEPT:LGNTPR interface. (*C*) Fluorescence polarization-based competition assays showing the decrease in polarization signal upon titration of unlabeled hInscPEPT into a mixture of LGNTPR and fluorescein-NuMAPEPT, or titration of unlabeled NuMAPEPT into a mixture of LGNTPR and fluorescein-hInscPEPT. (*D*) SEC analysis of the competitive interactions of Insc and NuMA1,807–1,987 with LGN:Gαi^{GDP}.

by the strong sequence conservation of the ortholog proteins in these regions (Fig. 2*E*, Fig. S5), equivalent mutations on hInscPEPT and dInscPEPT impair the association with the cognate LGNTPR and PinsTPR domains (Fig. 3 *F* and *G*). In particular, replacement of Trp31hInsc or of the glutamic acid couple E40-E42hInsc fully abrogates the interaction with LGNTPR. We next assessed the contribution of the conserved Asn203LGN, Arg221LGN, Arg235LGN, and Arg236LGN toward hInsc binding. Simultaneous substitution of Arg235LGN and Arg236LGN with alanine, as well as charge reversal of Arg236LGN to Glu severely perturbed the interaction, mirroring the effect observed for the corresponding PinsTPR mutations (Fig. 3*G*). Only upon replacement of Asn203LGN with a bulky phenylalanine we could score a binding reduction recapitulating the impairment observed with Asn226Pins. Finally, to evaluate whether equivalent chemical interactions sum up to similar overall binding affinities, we measured the strength of the binary interaction in both species by Isothermal Titration Calorimetry. The dissociation constants were 5 nM for the PinsTPR:dInscPEPT interaction and 13 nM for the LGNTPR:hInscPEPT one (Fig. S6). Collectively these results indicate that the LGN:Insc interface is evolutionary conserved.

NuMA Binds to LGN with an EPE-Motif. In mitosis the association of LGN with NuMA is fundamental to sustain the spindle orientation process. Previous studies have mapped the LGN-binding site of NuMA within a C-terminal portion of about 20 KDa encompassing residues 1,878–1,910 (18). This fragment of NuMA has been shown to enter a complex with LGNTPR, raising the question as to whether it is compatible with the concomitant presence of Insc on the same domain. Primary sequence analysis of NuMA revealed the existence of a conserved EPE motif at position 1,896–1,898, strongly suggesting that NuMA could interact with LGN with the same binding mode displayed by Insc (Fig. 4*A*). To test this hypothesis, we expressed NuMA1,886–1,914 (referred to as NuMAPEPT hereon) fused to a GST moiety, and checked its ability to interact with LGNTPR by GST pull-down assay. Indeed, NuMAPEPT binds LGNTPR in an EPE-dependent manner (Fig. 4*B*). Furthermore, all asparagine and arginine residues of LGNTPR found to be in contact with EPE motif of hInscPEPT are also important for NuMAPEPT recognition. Single substitutions on LGNTPR abrogate binding to NuMAPEPT due to the lower binding affinity displayed by NuMAPEPT for LGNTPR with respect to the one between hInscPEPT and LGNTPR, with dissociation constants of about 50 nM and 13 nM respectively (Fig. S6). We conclude that NuMAPEPT and hInscPEPT associate with LGNTPR via a conserved EPE motif.

NuMA and Insc Are Competitive Interactors of LGN. To ascertain whether hInscPEPT and NuMAPEPT are mutually exclusive interactors of LGNTPR, we developed a fluorescence polarization-based competition assay. Fluorescein-labeled NuMAPEPT at a concentration of 15 nM was mixed with 250 nM of LGNTPR. Based on their reciprocal affinity, under these conditions about 85% of the fluorescein-NuMAPEPT are in complex with LGNTPR (Fig. S7). We then titrated into the reaction increasing amounts of unlabeled hInscPEPT, and measured the residual fluorescein-NuMAPEPT polarization at steady-state. The monotonic decrease of the polarization signal upon hInscPEPT addition indicates that hInscPEPT effectively competes with NuMAPEPT, and implies that the simultaneous binding of the two peptides on LGNTPR is precluded (Fig. 4*C*). We confirmed this result by performing an analogous competition experiment in which we titrated unlabeled NuMAPEPT to compete the binding of fluorescein-labeled hInscPEPT to LGNTPR. The fourfold lower affinity displayed by NuMAPEPT towards LGNTPR with respect to the one of hInscPEPT predicts that higher doses of NuMAPEPT are required to fully displace hInscPEPT from LGNTPR. The shift observed in the NuMA-inhibited curve as compared to the Insc-inhibited one fully satisfies this prediction.

We next asked if the competition observed for the short NuMAPEPT and hInscPEPT peptides reflects a genuine inability of full-length Inscutable and NuMA to concomitantly enter a complex with LGN. We purified a homogeneous form of human LGN:Gαi^{GDP} from insect cells following a previously described colysis method (4). When injected on a SEC column, the LGN:Gαi^{GDP} complex elutes at an apparent molecular weight compatible with the expected 1:4 stoichiometry (Fig. 4*D*). We also adapted the purification protocol to generate an Insc:LGN:Gαi^{GDP} complex by coexpression of Insc and LGN in insect cells followed by colysis with Gαi. We then mixed LGN:Gαi^{GDP} and Insc:LGN:Gαi^{GDP} in roughly equimolar amounts and analyzed the sample by SEC. Despite the significant difference in the theoretical molecular weights caused by the presence of Insc, the two complexes coelutes in about the same fractions. To test the effect of NuMA, we additioned the LGN:Gαi^{GDP} plus Insc:LGN:Gαi^{GDP} mixture with a 20-fold

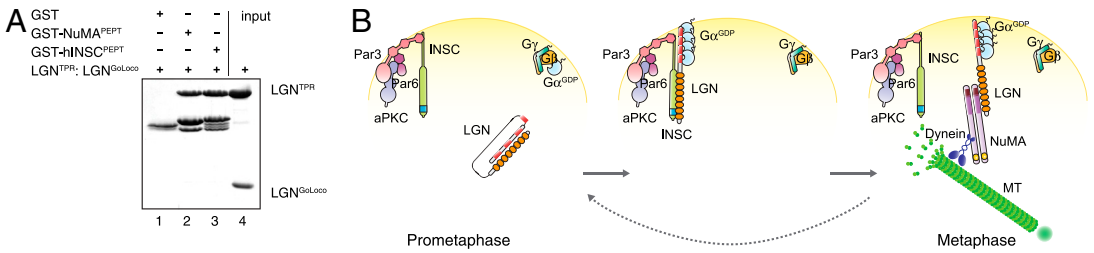

Fig. 5. Both NuMA and Insc open the LGN conformational switch. (*A*) Upon incubation of 2 μM GST-hInsc^{PEPT} with 4 μM of preformed LGN^{TPR}:LGN^{GoLoco}, only LGN^{TPR} is retained on beads, demonstrating that the simultaneous presence of LGN^{GoLoco} and Insc on the TPR domain is excluded. (*B*) Revised model of force generators functioning during asymmetric divisions.

molar excess of NuMA$^{1,807–1,987}$, and separated the resulting species by SEC. NuMA$^{1,807–1,987}$ readily bound to free LGN:Gαi^{GDP} and eluted in a well separated peak distinct from the Insc:LGN:Gαi^{GDP} one. In agreement with the competition model, the NuMA$^{1,807–1,987}$ excess was unable to dissociate Insc from LGN:Gαi^{GDP} due to its lower binding affinity. Of note, NuMA:LGN:Gαi^{GDP} elutes earlier than the Insc containing complex in spite of its smaller theoretical mass. We suspect that such behavior might be ascribed to specific hydrodynamical properties of the NuMA assembly, although we cannot rule out a dimerization of the NuMA-containing hetero-trimer. Collectively these findings demonstrate that Insc and NuMA utilize the ECE/EPE recognition motif to competitively associate with LGN.

Both NuMA and Insc Open the LGN Conformational Switch. One of the key events in the cortical force generators assembly is the release of the head-to-tail interactions holding LGN in an inhibited state. Previous studies have shown that the association of NuMA to LGN^{TPR} is capable of opening the conformational switch (3). Given the similarity in the binding mode of NuMA and Insc toward LGN^{TPR}, we enquired if Insc would also induce a similar conformational transition. To this end, we first reproduced the displacement the C-terminal LGN^{GoLoco} region from LGN^{TPR} observed upon NuMA addition (Fig. S8). We next took advantage of the stable LGN^{TPR}:LGN^{GoLoco} assembly mimicking the closed conformation of LGN to investigate the effect of Insc binding on the LGN conformational state. Our previous results proved that hInsc^{PEPT} forms a tight complex with LGN^{TPR}. When we repeated a similar GST pull-down experiment using LGN^{TPR}:LGN^{GoLoco} in solution, only the LGN^{TPR} half of the sandwich remained associated with the beads (Fig. 5*A*), providing compelling evidence that Insc opens the LGN switch. An analogous behavior is observed upon incubation of LGN^{TPR}:LGN^{GoLoco} with NuMA$^{1,807–1,987}$, that we included as a positive control.

Discussion

In this study we report the characterization of the Pins^{TPR}:dInsc^{PEPT} complex, and provide a molecular explanation for the mutual exclusive interaction of Insc and NuMA to LGN. While this manuscript was in preparation, Zhu and coworkers arrived to similar conclusions analyzing the structure of the LGN:NuMA complex (19).

A 38-residue fragment of *Drosophila* Insc encompasses the Pins^{TPR} binding region. This fragment of Insc shares a high sequence similarity to functional homologues recently discovered in mammals, fully supporting the notion that the basic mechanism responsible for the recruitment of force generators at polarity sites is evolutionary conserved. With the exception of a short N-terminal α-helix, the Insc^{PEPT} is intrinsically unstructured, and lines on the scaffold provided by the superhelical TPR arrangement of Pins with an extended conformation. The interaction surface is organized around a core module involving the EPE motif of Insc^{PEPT} and the central TPR5-6 of Pins, whose specificity is primarily dictated by charge complementarity. The binding is further stabilized by polar and hydrophobic interactions contributed by the αA helix of Insc^{PEPT}. Not surprisingly, the large interaction surface characterizing the topology of the Pins^{TPR}:Insc^{PEPT} heterotypic dimer accounts for an elevated binding affinity (of about 5 nM for the fly proteins and 13 nM for the human counterparts). The structure of mouse LGN$^{191–350}$, corresponding to what we name TPR5-8, with Insc$^{19–40}$ suggests that vertebrate proteins assemble with organizational principles similar to the fly ones (19). However, the short mouse constructs only depict the interaction of LGN^{TPR} with the αA helix of Insc^{PEPT}, up to the first Glu of the EPE motif. Intriguingly, the mouse LGN:Insc interaction seems to be characterized by lower affinity compared to human and fly ones (with K_D of 63 nM for LGN$^{TPR5–8}$:Insc$^{19–40}$, and of 47 nM for LGN$^{TPR1–8}$:Insc$^{20–57}$).

The evidence that NuMA forms a complex with the same LGN^{TPR} domain associating to Insc raised the question of whether it binds in a similar manner. Indeed, comparison of the primary sequence of Insc^{PEPT} with the known LGN-binding portion of NuMA revealed the presence of an EPE triplet that turned out to be essential for the LGN recognition, with a similar molecular signature of the EPE motif of the Insc^{PEPT}. Notably, the NuMA ortholog in fly (Mud) codes for two consecutive EDE-EGE motifs in the Pins-binding region, whose interplay remains to be clarified (Fig. S9). The structure of LGN in complex with NuMA^{PEPT} fully supports the notion that the EPE-interaction module represents a common region required for docking unstructured ligands on the LGN^{TPR} scaffold (19). In the case of NuMA, the interface is further contributed by a helical fragment forming a bundle with helices αA2 and αA3 of LGN^{TPR}. The consequence of the partial overlap between the Insc and NuMA binding sites is that their concomitant loading on LGN is excluded.

A key step during the assembly of the force generators is the opening of the LGN conformational switch that keeps the molecule in an inactive state (3). Binding of NuMA to LGN^{TPR} induces the release of the intramolecular interactions holding the molecule in a closed form. In agreement with the similarity in the binding modes, we demonstrated that also Insc disengages the LGN GoLoco motifs from the TPR domain. Together these findings imply that the GoLoco motifs contact the TPR repeats in the same region occupied by Insc and NuMA. Primary sequence inspection revealed that the GoLocos of both Pins and LGN do not contain EPE triplets, suggesting that either the head-to-tail interaction involves alternative TPR patches sterically occluded by the presence of Insc and NuMA, or that less conserved negatively charged triplets are accommodated on the same TPR5-6 of LGN.

The well established model for force generators recruitment at polarity sites rests on the assumption that Insc and NuMA can be part of the same apically localized multisubunit complexes containing Par proteins. This model stems from colocalization experiments showing that in asymmetric mitoses Par3, Insc, LGN, and NuMA cluster together in apical crescents (6), complemented by coimmunoprecipitation assays in which LGN:Gαi were found in association with Par3:Insc (12) and NuMA (18). The finding that Insc and NuMA are mutually exclusive partners of

LGN is both unexpected and puzzling. In particular, the higher affinity characterizing the Insc binding to LGN shifts the balance of the unmodified proteins towards the Insc:LGN complex formation, which is instrumental in recruiting LGN with Par proteins at the onset of mitosis but cannot account for microtubule-pulling forces. What is the possible mechanism for transferring LGN from Insc to NuMA? The architecture of the $Insc^{PEPT}$:$Pins^{TPR}$ structure whereby an extended ligand is accommodated on a large domain allows a high degree of regulation of the interaction strength. Posttranslational modifications on either side of the dimer might locally alter the contacts without affecting the rest of the interface, as it has been demonstrated for the similarly organized complex between the cytoplasmic domain of E-cadherin and β-catenin (17). Such modulating modifications can in principle occur on Insc, NuMA, or on LGN. To date, no experimental information is available regarding putative Insc or NuMA modifications. More controversial is the literature relative to LGN phosphorylations. In mitotic *Drosophila* neuroblasts, Pins has been found phosphorylated by Aurora-A on Ser436 at about half of the linker connecting the TPR domain with the GoLoco motifs (20). Using an "induced polarity" assay in S2 cells, phospho-$Ser436^{Pins}$ was shown to trigger a redundant NuMA-independent spindle orientation pathway engaging the membrane associated Dlg protein. It is to date unclear if such pathway is conserved in vertebrates. Notably, during oriented symmetric cell divisions of MDCK cells, phosphorylation on a similarly positioned Ser401 of LGN functions in excluding force generators from the apical cortex in order to prevent apico-basal spindle orientation (21). In this context, phospho-$Ser401^{LGN}$ would selectively prevent binding of LGN to apical Gαi. Based on our structural and biochemical results, it is difficult to provide a molecular explanation as to whether these LGN phosphorylations could also impact on the Insc and NuMA binding. Recent observations support the notion that the pool of NuMA:LGN:Gαi colocalizing with Par3:Insc in embryonic mouse skin progenitors is tightly regulated to set the balance between symmetric and asymmetric divisions, though no mechanism for this has been put forward (22). In summary, we reckon more has to be learnt to understand what brings LGN from Insc to NuMA.

An additional question relates to the mechanism maintaining effective NuMA:LGN:$G\alpha i^{GDP}$ species at the correct cortical sites in the absence of Insc. Based on the knowledge we acquired, we propose a step-wise model that can be schematized as follows (Fig. 5*B*): (*i*) in the early phases of mitosis LGN is brought to the apical membrane in conjunction with Par proteins by the high-affinity interaction with the preformed Par3:Insc complex. Binding of LGN to Insc triggers the conformational switch transition enabling the relocation of $G\alpha i^{GDP}$ moieties previously distributed all around the plasma-membrane with Gβγ; (*ii*) upon mitotic progression, when LGN is already at the correct sites, a yet unidentified molecular event alters the relative affinities of Insc and NuMA for LGN to shift the balance between the Insc-bound and the NuMA-bound LGN pools. We hypothesize that the four Gαi subunits present on LGN at this stage are sufficient to transiently hold cortical NuMA:LGN:$G\alpha i^{GDP}$ in proximity of Par proteins to allow directional microtubule pulling. We speculate that NuMA:LGN:$G\alpha i^{GDP}$ is a short-lived complex and disassemble, possibly assisted by a specialized GEF for Gαi such as as Ric-8A (23), releasing apo-LGN in the cytoplasm to start a new cycle. Such a dynamical interaction network would allow for a continuous regulation of the force exerted on astral microtubules throughout mitosis. Future attempts to validate the model in vivo will greatly benefit from the biochemical tools presented in this study.

Experimental Procedures

Detailed descriptions of crystallization, structure determination, and other experimental procedures are available in the *SI Materials and Methods*. Atomic coordinates and structure factors for the Pins:Insc structure have been deposited to the Protein Data Bank under accession code 4A1S.

ACKNOWLEDGMENTS. M.M. is funded by the Italian Association for Cancer Research (AIRC), and the Italian Ministry of Health. S.C. and A.A. are FIRC postdoctoral fellows.

1. Morin X, Bellaiche Y (2011) Mitotic spindle orientation in asymmetric and symmetric cell divisions during animal development. *Dev Cell* 21:102–119.
2. Knoblich JA (2010) Asymmetric cell division: recent developments and their implications for tumour biology. *Nat Rev Mol Cell Biol* 11:849–860.
3. Du Q, Macara IG (2004) Mammalian Pins is a conformational switch that links NuMA to heterotrimeric G proteins. *Cell* 119:503–516.
4. Tall GG, Gilman AG (2005) Resistance to inhibitors of cholinesterase 8A catalyzes release of Galphai-GTP and nuclear mitotic apparatus protein (NuMA) from NuMA/LGN/Galphai-GDP complexes. *Proc Natl Acad Sci USA* 102:16584–16589.
5. Merdes A, Heald R, Samejima K, Earnshaw WC, Cleveland DW (2000) Formation of spindle poles by dynein/dynactin-dependent transport of NuMA. *J Cell Biol* 149:851–862.
6. Williams SE, Beronja S, Pasolli HA, Fuchs E (2011) Asymmetric cell divisions promote Notch-dependent epidermal differentiation. *Nature* 470:353–358.
7. Kraut R, Chia W, Jan LY, Jan YN, Knoblich JA (1996) Role of inscuteable in orienting asymmetric cell divisions in *Drosophila*. *Nature* 383:50–55.
8. Kraut R, Campos-Ortega JA (1996) Inscuteable, a neural precursor gene of *Drosophila*, encodes a candidate for a cytoskeleton adaptor protein. *Dev Biol* 174:65–81.
9. Yu F, Morin X, Cai Y, Yang X, Chia W (2000) Analysis of partner of inscuteable, a novel player of *Drosophila* asymmetric divisions, reveals two distinct steps in inscuteable apical localization. *Cell* 100:399–409.
10. Schaefer M, Shevchenko A, Shevchenko A, Knoblich JA (2000) A protein complex containing Inscuteable and the Galpha-binding protein Pins orients asymmetric cell divisions in *Drosophila*. *Curr Biol* 10:353–362.
11. Zigman M, et al. (2005) Mammalian inscuteable regulates spindle orientation and cell fate in the developing retina. *Neuron* 48:539–545.
12. Lechler T, Fuchs E (2005) Asymmetric cell divisions promote stratification and differentiation of mammalian skin. *Nature* 437:275–280.
13. Konno D, et al. (2008) Neuroepithelial progenitors undergo LGN-dependent planar divisions to maintain self-renewability during mammalian neurogenesis. *Nat Cell Biol* 10:93–101.
14. Das AK, Cohen PW, Barford D (1998) The structure of the tetratricopeptide repeats of protein phosphatase 5: implications for TPR-mediated protein-protein interactions. *EMBO J* 17:1192–1199.
15. Jinek M, et al. (2004) The superhelical TPR-repeat domain of O-linked GlcNAc transferase exhibits structural similarities to importin alpha. *Nat Struct Mol Biol* 11:1001–1007.
16. Conti E, Uy M, Leighton L, Blobel G, Kuriyan J (1998) Crystallographic analysis of the recognition of a nuclear localization signal by the nuclear import factor karyopherin alpha. *Cell* 94:193–204.
17. Huber AH, Weis WI (2001) The structure of the beta-catenin/E-cadherin complex and the molecular basis of diverse ligand recognition by beta-catenin. *Cell* 105:391–402.
18. Du Q, Stukenberg PT, Macara IG (2001) A mammalian partner of inscuteable binds NuMA and regulates mitotic spindle organization. *Nat Cell Biol* 3:1069–1075.
19. Zhu J, et al. (2011) LGN/mInsc and LGN/NuMA complex structures suggest distinct functions in asymmetric cell division for the Par3/mInsc/LGN and Galphai/LGN/NuMA pathways. *Mol Cell* 43:418–431.
20. Johnston CA, Hirono K, Prehoda KE, Doe CQ (2009) Identification of an Aurora-A/PinsLINKER/Dlg spindle orientation pathway using induced cell polarity in S2 cells. *Cell* 138:1150–1163.
21. Hao Y, et al. (2010) Par3 controls epithelial spindle orientation by aPKC-mediated phosphorylation of apical Pins. *Curr Biol* 20:1809–1818.
22. Poulson ND, Lechler T (2010) Robust control of mitotic spindle orientation in the developing epidermis. *J Cell Biol* 191:915–922.
23. Woodard GE, et al. (2010) Ric-8A and Gi alpha recruit LGN, NuMA, and dynein to the cell cortex to help orient the mitotic spindle. *Mol Cell Biol* 30:3519–3530.